Int. Conference on Boundary and Interior Layers
BAIL 2006
G. Lube, G. Rapin (Eds)

Detached Eddy Simulation of Supersonic Shear Layer Wake Flows

H. Lüdeke, V. Togiti

DLR, Institute of Aerodynamics and Flow Technology
Lilienthalplatz 7, D-38108 Braunschweig
Heinrich.Luedeke@dlr.de

1. Introduction

The modelling of unsteady side loads induced by the interaction of flow separation in the wake of hypersonic re-entry vehicles play an important role for the design of such systems. The simulation of these phenomena is one of the main challenges during descent especially for re-entry capsules. To investigate the turbulent wake flow, basic studies of generic configurations and the applicability of advanced turbulence modelling are necessary. For this reason validations of Detached Eddy Simulation [1] for an axisymmetric supersonic cylinder configuration at $M_\infty = 2.4$ are carried out to earn experience for unsteady simulations of re-entry vehicles. Detached-eddy simulation is a hybrid approach for the modelling of turbulent flow fields at complex geometries. The idea is to combine the best features of both, the Reynolds-averaged Navier-Stokes (RANS) and the large eddy simulation (LES) approach to predict massively separated unsteady flow fields at high Reynolds-numbers especially in the wake of Re-entry vehicles during descent. In this study the Spalart-Allmaras one-equation turbulence model [2] is used as an accurate and efficient base for DES.
The intention of the current work is the investigation of the unsteady axisymmetric flow fields. The typical time averaged flow field for this configuration is shown in Figure 1 with pressure contours and streamlines. The large turning angle behind the base causes separation and a region of reverse flow as visible in the wake. The point along the axis of symmetry where the streamwise velocity is zero is considered to be the shear layer reattachment point. In this region the flow is forced to turn along the axis of symmetry causing a reattachment shock to be formed. The detailed experimental data base, provided by Herrin and Dutton [3], is used for comparison of numerically predicted and measured turbulent data. The practical applicability of the approach is demonstrated considering as an example an axisymmetric re-entry capsule at a hypersonic Mach number of $M_\infty = 5.1$ under free flight conditions. All simulations were carried out by the hybrid structured-unstructured DLR-τ-code which is extensively validated for sub- trans- and hypersonic cases as well as for various RANS and DES simulations [4]. For the axisymmetric cylinder-configuration structured and unstructured grids have been generated at different resolution of the turbulent wake. They are designed with a similar resolution used by Forsythe and Sqires in [5]. Especially the near wake of the cylinder is refined extensively, following the recommendation of Spalart [1]. Aside from grid studies, investigations of different low-Reynolds number modifications of the LES part proposed by Breuer [6] were applied for both grids. With these improvements it was possible to resolve significantly refined turbulent structures with the same grid resolution. In the wake the turbulent kinetic energy and turbulent intensities in radial and streamwise direction, computed by extracting the standard deviation of the velocities over the time, was successfully compared with the measurements. Furthermore the pressure level along the base was compared with the experimental pressure distribution at the cylinder-base [3]. Finally simulations of a realistic re-entry capsule, designed as a recovery orbital platform [7], are carried out to give a practical demonstration of DES modelling for hypersonic flight. To ensure the turbulent wake flow a trajectory point at $M_\infty = 5.1, Re = 20 \cdot 10^6$

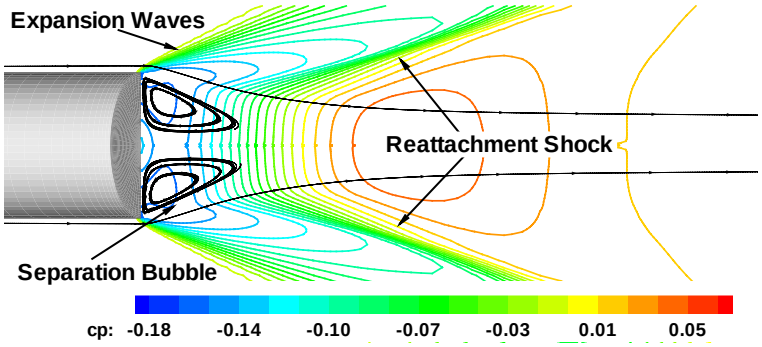

Figure 1: flow topology of axisymmetric base flow and Cp distribution

was chosen. The influence of different DES modifications on the resolution of the turbulent flow field was investigated for this vehicle.

2. Numerical simulation tools

The CFD computations for this study are performed with the hybrid structured/unstructured DLR-Navier-Stokes Solver τ [4]. The τ-code is a second order finite-volume flow solver for the Euler and Navier-Stokes equations in the integral form. Different numerical schemes like cell-centred for sub- and transsonic flow and AUSMDV for super- and hypersonic flow conditions are implemented. Second-order accuracy for upwind schemes is obtained by the MUSCL extrapolation, in order to allow the capturing of strong shocks and contact discontinuities. A three-stage Runge-Kutta as well as an implicit LUSGS scheme is available to advance the solutions in time for steady flow fields. For acceleration of the convergence local time stepping, implicit residual smoothing and full multigrid are optional. For fast and accurate transient flow simulations a dual time stepping scheme, following Jameson is implemented, which is an implicit algorithm and not restricted in the choice of the smallest timestep in the flow field. To overcome this limit the time derivative in the Navier-Stokes equations is discretized by a second order backwards difference, resulting in a non-linear equation system which converges towards the subsequent timestep by using an inner pseudo-time. Within this inner loop all mentioned acceleration techniques such as local time stepping and residual smoothing are applicable. With this approach an acceleration of time accurate calculations of 2^{nd} up to 3^{rd} order is possible. Several one- and two equation turbulence models are available for steady simulations. In the presented RANS-cases the one-equation Spalart-Allmaras (SA) model is used which is briefly described in the Investigation of Unsteady Loads due to Turbulent Supersonic wake Flow following. The model defines the eddy viscosity field as

$$\mu_t = \rho\nu_t = \rho\tilde{\nu} f_{\nu 1} \tag{1}$$

with ρ as the density, ν_t as the turbulent kinematic viscosity and $f_{\nu 1}$ as a near wall-function that guarantees linear behaviour of the turbulent transport quantity near walls:

$$f_{\nu 1} = \left(\frac{\chi^3}{\chi^3 + c_{\nu 1}^3}\right), \chi = \frac{\tilde{\nu}}{\nu} \tag{2}$$

with ν as the molecular viscosity. The distribution of the transport quantity$\tilde{\nu}$ is determined by the solution of

$$\frac{D(\rho\tilde{\nu})}{Dt} = \underbrace{c_{b1}\tilde{S}\rho\tilde{\nu}}_{P} - \underbrace{c_{w1} f_w \rho \left(\frac{\tilde{\nu}}{d}\right)^2}_{D} + \underbrace{\frac{\rho}{\sigma}\left\{\nabla\left[(\nu+\tilde{\nu})\nabla\tilde{\nu}\right] + c_{b2}(\nabla\tilde{\nu})^2\right\}}_{DF} \tag{3}$$

with d as the wall distance. This transport equation contains phenomenological models of production P, destruction D and diffusion DF. The destruction term D is needed to model the blocking effects near walls. In the production term P a modified vorticity $\tilde{S}$ appears that maintains the linear behavior of the model near walls:

$$\tilde{S} = S + \frac{\tilde{\nu}}{k^2 d^2} f_{\nu 2},\ f_{\nu 2} = 1 - \frac{\chi}{1 + \chi f_{\nu 1}} \tag{4}$$

The function $f_{\nu 2}$ is constructed in a way that the vorticity S maintains its log-layer behavior all the way to the wall. The destruction term

$$D = c_{w1} f_w \rho \left(\frac{\tilde{\nu}}{d}\right)^2 \tag{5}$$

is constructed by using the wall function f_w:

$$f_w = g \left[\frac{1 + c_{w3}^6}{g^6 + c_{w3}^6}\right]^{1/6} \tag{6}$$

$$g = r + c_{w2}\left(r^6 - r\right) \tag{7}$$

$$r = \frac{\tilde{\nu}}{\tilde{S} k^2 d^2} \tag{8}$$

The different model constants $c_{\nu 1}, c_{b1}, c_{b2}, c_{w1}, c_{w3}$ are determined by experimental data and analytical solutions and are well known for turbulent flow fields [2]. Within the last years more recent turbulence models like DES are implemented [1]. DES is a hybrid RANS-LES approach that bases on a modification of the wall distance term in the SA model. While RANS is used in the unsteady boundary layer flow with a standard grid resolution where it performs reasonable results, LES is used in separated regions where relevant turbulent scales can be modeled. The switching between RANS and LES bases on a characteristic length scale, chosen to be proportional with Δ which is the largest cell dimension:

$$\Delta = max(\Delta x, \Delta y, \Delta z) \tag{9}$$

For the standard DES formulation the wall distance d in the SA model is replaced by where $\tilde{d}$ is defined as:

$$\tilde{d} = min(d, c_{DES}\Delta) \tag{10}$$

with C_{DES} as a constant calibrated by using isotropic turbulence. In this mode a local equilibrium between production and destruction term in the SA model is expected. This local balance leads to the relation $\tilde{\nu} \propto \tilde{S} \cdot \tilde{d}^2$ which is very similar to the relationin the Smagorinsky model, namely $\nu_t \propto S \cdot d^2$. Consequently the only difference between SA-DES in LES-mode and the original Smagorinsky model lies in the SA-wall-functions $f_{\nu 1}, f_{\nu 2}, f_w$, hidden in $\tilde{\nu}$ and $\tilde{S}$. The influence of these functions in the original wall functions is small for high Reynolds numbers, and disappears for a large wall distance. However in LES mode the wall distance is substituted by the small filter width, so the impact of these functions especially in free shear flow can be significant. In order to get the exact Smagorinsky model, Breuer [6] expected the following conditions to be satisfied in the LES region ($d > C_{DES}\Delta$) :

$$\begin{aligned} f_{\nu 1} &= 1 \\ f_{\nu 2} &= 0 \\ f_w &= 1 \end{aligned} \tag{11}$$

These functions can be easily included in the original DES formulation, and the modification is optional in the recent τ-code version. The impact on the investigated validation cases will be shown for the axisymmetric wake flow.

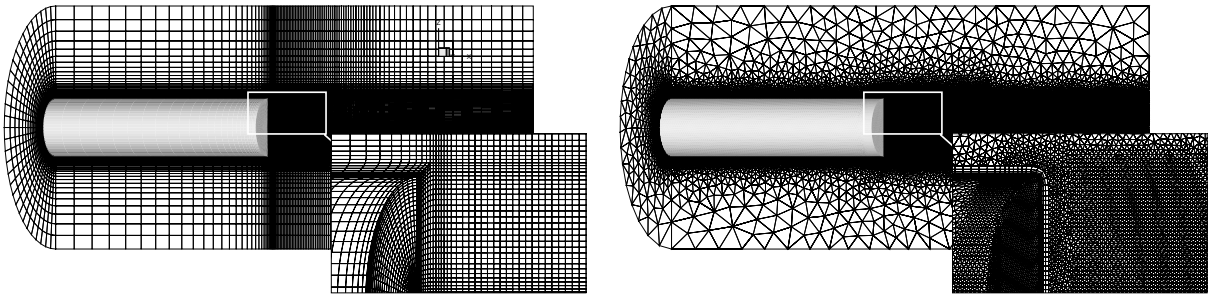

Figure 2: Hexahedral and tetrahedral grid for the cylinder wake

3. Grid generation

For basic studies of compressible DES a coarse hexahedral grid with axisymmetric character, shown at the left hand side of Figure 2, is generated. The cell distribution is inspired by the work of Forsythe [5] and Spalart [1]. For grid convergence studies also a hybrid unstructured grid is used (Figure 2 right part) while the hexahedral grid has only 360.000 cells, to study the accuracy of the numerical schemes, the hybrid grid with about 2.000.000 cells provides a significantly improved resolution in the shear layer and wake, but on the other hand an increase in computational time. The Hexahedral grid for the capsule configuration was designed with the experience gained from the cylinder simulations (Figure 3). To earn computational costs the grid was subdivided into a forebody, where steady simulations are carried out, and a cylindrical afterbody for DES with a fixed inflow plane, given by the calculation of the first part.

4. Computational results

4..1. Axisymmetric base flow

For both grids the standard DES model, suggested by Spalart [1] with a slightly modified filter-length is used. Instead of the maximum cell diameter the third root of the cell volume, typically used for LES simulations, is chosen in the DES-region, defined by the standard procedure. The advantage of this choice is a better treatment of highly stretched cells in hexahedral grids. It has to be noted, that the switching between RANS and LES is kept at the same position as before, so the whole boundary layer is still computed in RANS-mode. The test conditions for the compressible base flow are taken from [5] at $M_\infty = 2.46, Re_\infty = 45 \cdot 10^6/m, U_\infty = 593.8m/s$

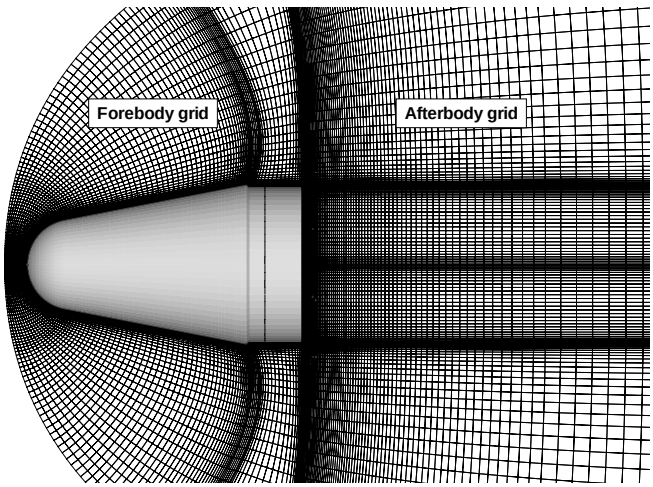

Figure 3: Fore- and afterbody grid of the re-entry capsule.

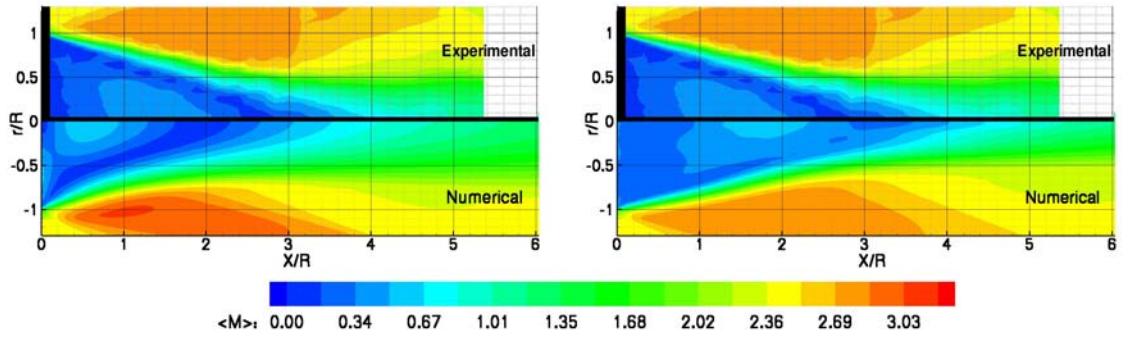

Figure 4: Averaged Mach contours behind cylinder base. Left: RANS on hexahedral grid, right: averaged Mach contour of DES . Experimental part taken from [1].

and a cylinder radius R of 31.75 mm. The averaged Mach number distribution in the cylinder wake agrees well with the experimental data by Herrin and Dutton [3], as shown in Figure 4 for RANS and DES simulation. For this insensitive quantity even steady RANS simulations show reasonable results, although the agreement with DES is much better. Also higher statistical moments, like the resolved turbulent kinetic energy $k = 0.5\left(\sigma u^2 + \sigma v^2 + \sigma w^2\right)$ are compared, where $\sigma u, \sigma v, \sigma w$ are the standard deviations over the time of the velocity components. The result of k for the standard DES model is shown in Figure 5 on the left hand side with the same k-distribution in the shear layer. The results could be improved by using the refined unstructured grid, as shown on the right hand side. With the improved resolution of the free shear layer it is possible to get a much better agreement of the k-distribution in that region as expected physically. Basically the same result is valid for the turbulent intensities (Figure 6). For the hexahedral grid the resolution of the shear layer in front of x/R = 3 is still insufficient. For the tetrahedral grid the maximum is moving upstream although the values are still too large in the farfield of the wake. Another investigation of the simulations with the unstructured grid is the fact, that a full resolution of the turbulent elements in the shear layer requires further refined grids. This deficiency results usually in a non symmetric separation which is still present in the time averaged output, although it is of course diminished. As a remedy for this phenomenon, which is also reported by Forsythe in [5], further refined grids especially in the shear layer region and adaptation techniques for this kind of flowfield are an objective of ongoing work.
To improve the results on the coarse grid especially in the subsonic separation region, also a modification of the standard model, proposed by Breuer [6] is tested. The advantage of this formulation, that reduces the dissipation of the DES, is visible in Figure 7, where computations

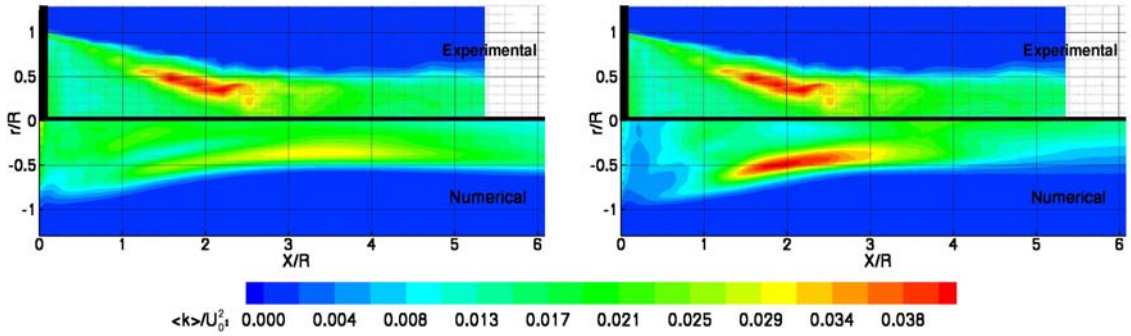

Figure 5: Resolved turbulent kinetic energy behind the cylinder base. Left: DES on hexahedral grid, Right: DES on tetrahedral grid. Experimental part taken from [5].

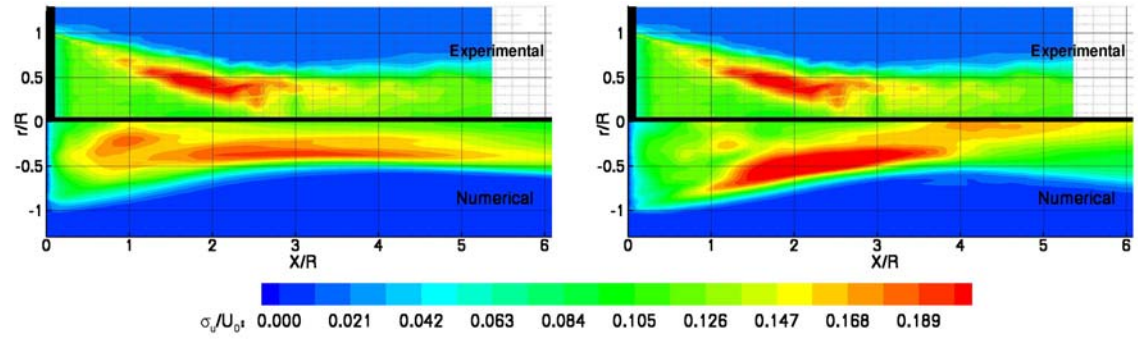

Figure 6: Streamwise turbulent intensity behind the cylinder base. Left: DES on hexahedral grid, Right: DES on tetrahedral grid. Experimental part taken from [5].

on the hexahedral grid with both DES modifications are shown. The finer resolution of the turbulent structures in the vorticity is clearly visible. Main advantages of the DES-approach are shown by a comparison between simulated and experimental pressure distribution at the cylinder-base and the centerline velocity for RANS- and DES-calculations (Figure 8). As visible the mean pressure level predicted by RANS is globally smaller than the experimental data while the DES results generated on the hexahedral grid with DES agree much better with the experiments. Even slightly better results are obtained from the tetrahedral grid. This is also true for the centreline velocity where in the near wake hexa- and tetrahedral grid solutions show good results while in the far wake obviously the significantly higher resolution of the tetrahedral grid is necessary to get the exparimental velocity level. especially the re-attachment is resolved quite well.

4..2. Cylindrical re-entry capsule

To give a practical demonstration of DES modelling in the hypersonic regime, turbulent simulations are performed at the wake flow of a realistic re-entry capsule, a facility conceived to be a recovery platform to perform orbital flights. For these simulations the computational axisymmetric hexahedral grid was subdivided into a forebody, where steady simulations are carried out, and a cylindrical afterbody for DES with a fixed inflow plane, given by the calculation of the first part. To ensure turbulent wake flow a trajectory point at $M_\infty = 5.1, Re_\infty = 20 \cdot 10^6$ was chosen. Free-flight conditions are expected and radiative equilibrium is chosen as a wall boundary condition. A snapshot of the vorticity contours in this region is shown in Figure 9, also with and without Breuer modification. As visible, the resolution of the turbulence elements has the same quality reached for the cylinder-case and the Breuer modification increases the resolution significantly as well.

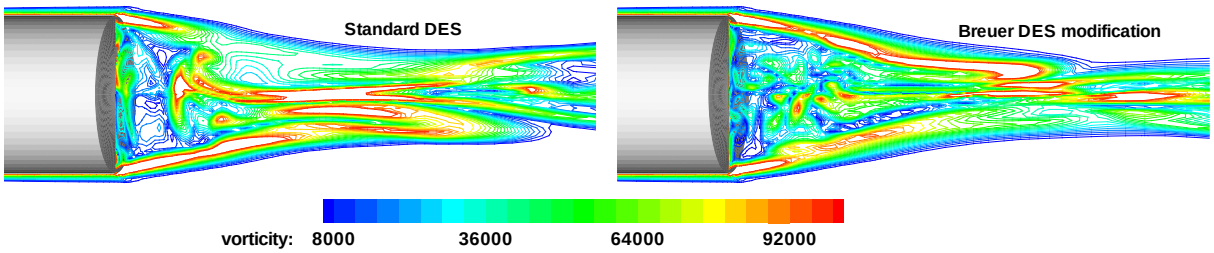

Figure 7: Vorticity in the cylinder wake for different DES modifications on the hexahedral grid.

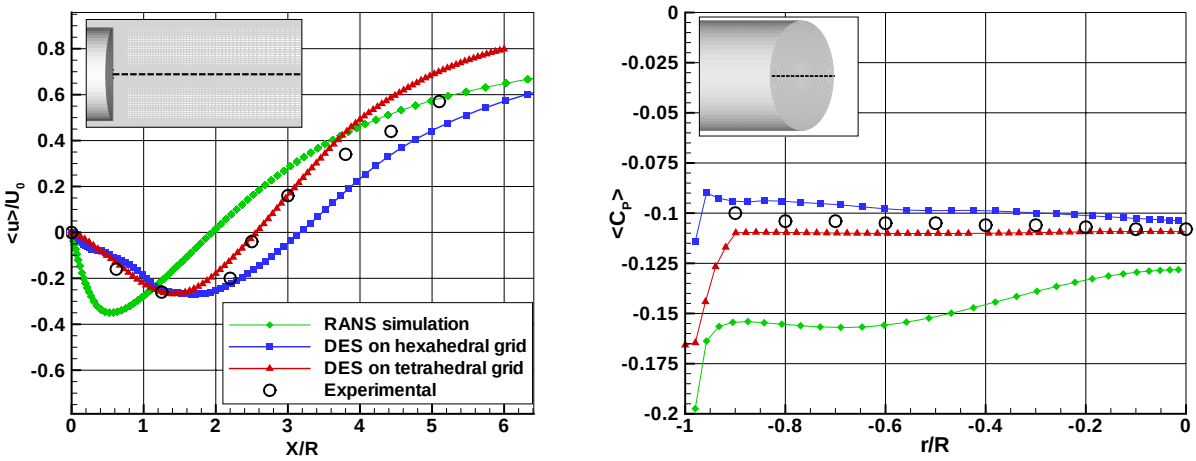

Figure 8: Averaged centerline velocity and pressure along the base for different turbulence models on the structured grid.

5. Conclusion

The present study investigates unsteady axisymmetric flow fields in the wake of a blunt cylinder at $M_\infty = 2.4$ and a cylindrical re-entry capsule under hypersonic flight conditions of $M_\infty = 5.1$. These time accurate Detached Eddy Simulations have shown very good comparability with experimental data especially for the prediction of the base pressure. Also other turbulent quantities like the diagonal elements of the Reynolds-stress tensor and the turbulent kinetic energy compare well with the measured data. Finally the technique was applied on a realistic Re-entry capsule to emphasise the applicability of the new technique for super- and hypersonic flows of re-entry vehicles. First simulation results are shown for this configuration. The results agree well with the flowfield obtained by the cylinder test-case.

References

[1] P.R. Spalart, "Young-Persons Guide to Detached- Eddy Simulation Grids", *NASA/CR-2001-211032*, (2001).

[2] P.R. Spalart, S.R. Allmaras, "A One Equation Turbulence Transport Model for Aerodynamic Flows", *La Recherche Aerospaciale*, **1**, 5–21 (1994).

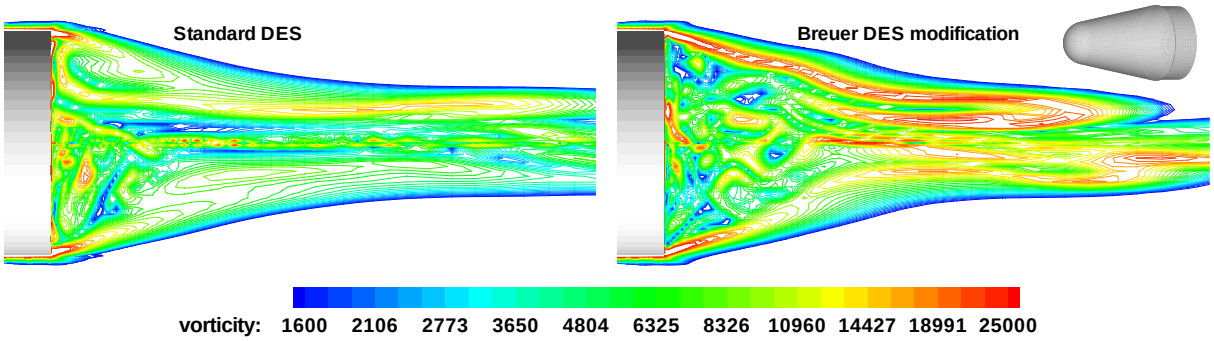

Figure 9: Instantaneous vorticity contours in the capsule wake for different DES modifications on the hexahedral grid at $M_\infty = 5.1$, $Re = 20 \cdot 10^6$.

[3] J.L. Herrin, J.C. Dutton, "Supersonic Base flow Experiments in the Near Wake of a Cylindrical Afterbody", *AIAA Journal*, **3**2-1, xxx-yyy (1994).

[4] A. Mack, V. Hannemann, "Validation of the unstructured DLR-TAU-Code for Hypersonic Flows", *AIAA 2002-3111*, (2002).

[5] J.R. Forsythe, K.A. Hoffmann, K.D. Squires, "Detached-Eddy Simulation with compressibility Corrections Applied to a Supersonic Axisymmetric Base Flow", *AIAA 2002-0586*, (2002).

[6] M. Breuer, N. Jovicic, K. Mazaev, "Comparison of DES, RANS and LES for the separated flow around a flat plate at high incidence", *Int. J. Numer. Meth. Fluids*, **41**, 357–388 (2003).

[7] Alessandro La Neve, Flavio de Azevedo Correa Junior, "SARA Experiment Module Project: Using Skills to Enlarge Experiences", *International conference on Engineering Education, Manchester, U.K.*, August 18-21 (2002).